MEDICAL SCIENCE MONITOR BASIC RESEARCH

HUMAN STUDY

e-ISSN 2325-4416
© Med Sci Monit Basic Res, 2019; 25: 33-44
DOI: 10.12659/MSMBR.913436

Received: 2018.10.01
Accepted: 2018.12.21
Published: 2019.02.04

Autophagy and Oncosis/Necroptosis Are Enhanced in Cardiomyocytes from Heart Failure Patients

Authors' Contribution:
Study Design A
Data Collection B
Statistical Analysis C
Data Interpretation D
Manuscript Preparation E
Literature Search F
Funds Collection G

ABCDEFG 1 Giovanni Corsetti*
ABCDEF 2 Carol Chen-Scarabelli*
BCDF 3 Claudia Romano*
CD 4 Evasio Pasini
CE 5 Francesco S. Dioguardi
BD 6 Francesco Onorati
BCEF 7 Richard Knight
B 8 Hemang Patel
CE 9 Louis Saravolatz#
BCE 6 Giuseppe Faggian#
ABCDEFG 2 Tiziano M. Scarabelli#

1 Division of Human Anatomy and Physiopathology, Department of Clinical and Experimental Sciences, University of Brescia, Brescia, Italy
2 Center for Heart and Vessel Preclinical Studies, Department of Internal Medicine, St. John Hospital and Medical Center, Wayne State University, Detroit, MI, U.S.A.
3 Department of Clinical and Experimental Sciences, University of Brescia, Brescia, Italy
4 Scientific Clinical Institutes Maugeri, Cardiac Rehabilitation Lumezzane Institute, Brescia, Italy
5 Department of Internal Medicine, University of Cagliari, Cagliari, Italy
6 Division of Cardiovascular Surgery, Verona University Hospital, Verona, Italy
7 Medical Research Council (MRC) Toxicology Unit, University of Cambridge, Cambridge, United Kingdom
8 General Medical Education, Department of Internal Medicine, Ascension St. John Hospital, Detroit, MI, U.S.A.
9 Department of Medicine, Ascension St John Hospital and Wayne State University School of Medicine, Detroit, MI, U.S.A.

* Giovanni Corsetti, Carol Chen-Scarabelli and Claudia Romano equally contributed to this work
# Louis Saravolatz, Giuseppe Faggian and Tiziano M. Scarabelli equally contributed as senior authors to the manuscript

Corresponding Author: Giovanni Corsetti, e-mail: giovanni.corsetti@unibs.it
Source of support: The work was sponsored by a grant provided by St. John Guild Foundation to CCS and TS and by a grant provided by Dolomite-Franchi S.p.a. (Marone-Brescia, Italy) to GC

Background: Although originally described as a survival mechanism, it is unknown whether and to what extent autophagy is implicated in the terminal stages of heart failure. Here, we studied magnitude and evolution of autophagy in patients with intractable heart failure.

Material/Methods: Myocardial samples were obtained from 22 patients with ischemic cardiomyopathy and idiopathic dilated cardiomyopathy who were undergoing cardiac transplantation. Hearts from 11 patients who died from non-cardiac causes were used as control samples. Autophagy was evaluated by immunostaining with a monoclonal microtubule associated protein light chain 3 (LC3)-II antibody, while the relationship of autophagy with apoptosis and oncosis was assessed by double staining with TUNEL (terminal deoxynucleotidyl transferase – mediated deoxyuridine triphosphate nick end labeling) assay and complement 9 (C9) immunological staining, respectively. In addition, several necroptotic markers, including RIP1 and RIP3 (receptor interacting protein kinase 1 and 3), anti-C3 (cleaved-caspase-3), and anti-NF-κB (nuclear factor kappa-light-chain-enhancer of activated B cells) were assessed by immunohistochemistry.

Results: Anti-LC3-II staining was detected in 8.7±1.6% of the heart failure patient heart samples and in 1.2±0.3% of control patient heart samples. Vacuole formation started at one nuclear pole, before becoming bipolar and involving the cytosol. Subsequently, the autophagic process extended also to the nuclei, which underwent a progressive vacuolization and disintegration, assuming a peculiar "strawberry like appearance". Myocytes with extensive vacuole formation exhibited nuclear degeneration, which was associated with TUNEL, C3, C9, RIP1, and RIP3 positive staining. Conversely, myocytes with less extensive vacuole formation showed RIP1 and NF-κB positive staining, though not positivity for other cell death markers.

Conclusions: Autophagy was extensively detected in end-stage heart failure and its progression, resulted in secondary cell death, with occurrence of oncosis and necroptosis exceeding that of apoptosis. Conversely, activation of the RIP1/NF-κB pathway was associated with cell survival.

MeSH Keywords: Apoptosis • Autophagy • Heart Failure

Full-text PDF: https://www.basic.medscimonit.com/abstract/index/idArt/913436

3717 2 8 41

Indexed in: [Index Medicus/MEDLINE] [EMBASE/Excerpta Medica] [Chemical Abstracts/CAS]

Background

Myocyte cell loss is an important mechanism in the development of heart failure. Although the traditional explanation for myocytes cell loss has been accidental cell death, lately there has been a surge of evidence affirming the role of apoptotic cell death [1]. More recently, other causes of cell loss have been reported. Indeed, besides necrosis and apoptosis, autophagy has also been reported to occur in cardiac myocytes [2] and has been recognized to play a role in the pathophysiology of human heart failure [3–5], as well as in ischemia-reperfusion injury [6,7]. Notably, recent findings have suggested that the occurrence of autophagy enhanced the survival of cardiac cells in hearts exposed to permanent coronary artery occlusion [6].

Macroautophagy (hereafter referred to as autophagy) is a process of intracellular bulk degradation in which cytoplasmic components, including organelles, are sequestered within double-membrane vesicles (autophagosomes) and finally delivered to the lysosome for degradation [8,9]. Autophagy has long been known to be a physiological mechanism of cell survival during periods of temporary starvation, and has, for example, been observed in mice between birth and suckling [10]. As such, it may also occur during brief periods of ischemia [11]. Indeed, autophagosomes and autophagy have been observed in rabbit hearts exposed to 20 to 40 minutes of simulated ischemia followed by reperfusion [12], and this was associated with recovery of myocyte function. Surprisingly, except for isolated reports [13], the subsequent literature has paid little attention to autophagy as a cell protective mechanism in the ischemic myocardium.

Despite the most recent advances in understanding the molecular mechanisms and biological functions of autophagy [11], it is currently uncertain whether autophagy acts primarily as a cell survival mechanism versus a cell death pathway or both under different conditions. In the case of a shortage of intracellular nutrients secondary to starvation/growth factor withdrawal or impaired adenosine triphosphate (ATP) synthesis in the setting of ischemia, autophagy may help promote cell survival, either by purging the cell of damaged organelles, or by generating the intracellular building blocks required to maintain vital functions, which finally results in ATP production, macromolecular synthesis, and improved cell survival [14]. Under more extreme conditions, autophagy may also promote cell death through excessive self-digestion and degradation of essential cellular constituents. There are 16 proteins participating in the autophagy pathway in man. The autophagy light-chain-3 protein (LC3), a mammalian homologue of Atg8, was originally identified as microtubule-associated protein [15]. LC3 is the only known mammalian protein, which stably associates with the autophagosome membranes and is commonly used as a sensitive marker for detecting autophagy in mammalian cells. Although originally described as a survival pathway against stressful events, whether and to what extent autophagy is implicated in the terminal stages of heart failure is unknown.

Accidental cell death with swelling, namely oncosis, is the main type of cell demise documented in known models of ischemic injury [16]. Complement 9 (C9), a part of the membrane attacking complex C5b-9, is a member of the complement membrane attack complex (MAC) that forms transmembrane channels. These channels disrupt the cell membrane of target cells, leading to cell lysis and death [17]. For this reason, C9 is considered a useful tool for detection of early oncosis [18].

Necroptosis is a well-characterized cell damaging process, combining morphological features of accidental cell death and maladaptive autophagy. Indeed, necroptosis involves loss of membrane integrity and release of damage-associated molecular pattern molecules (DAMPs), resulting in secondary inflammatory response [19]. Biochemically, necroptosis is a programmed process orchestrated by a complex set of proteins involving receptor-interacting protein kinase 1 and 3 (RIP1, RIP3), as well as mixed lineage kinase domain-like protein (MLKL). Activation of the RIP1-RIP3-MLKL signaling pathway leads to disruption of cation homeostasis, plasma membrane rupture, and finally cell death [20].

Nuclear factor kappa-light-chain-enhancer of activated B cells (NF-κB) is a redox-regulated transcription factor involved in inflammation, immune function, cellular proliferation [21], apoptosis [22], and anti-apoptotic activities [23]. The nature of the signals elicited by death inducers determines whether NF-κB induction leads to apoptosis or survival [24].

Because heart failure patients commonly have high levels of inflammation [25], we hypothesized that cardiomyocytes could be damaged primarily by autophagy and/or oncosis/necroptosis rather than apoptosis. Hence, the aim of the present study was to evaluate the magnitude and progression of autophagy and the simultaneous presence of oncosis/necroptosis and apoptosis in patients with intractable heart failure by immunohistochemistry (IHC) using anti-LC3-II, anti-C9, anti-RIP1, anti-RIP3, anti-NF-κB, TUNEL (terminal deoxynucleotidyl transferase–mediated deoxyuridine triphosphate nick end labeling), and anti-C3 (cleaved caspase-3) antibodies, and electron microscopy (EM) morphology.

Material and Methods

Patient population

The work has been carried out in accordance with The Ethics Code of the World Medical Association (Declaration of Helsinki).

Indexed in: [Index Medicus/MEDLINE] [EMBASE/Excerpta Medica] [Chemical Abstracts/CAS]

Table 1. Demographical, clinical, anatomical, and functional characteristics of heart failure patients.

Variable	Female (n=7)	Male (n=15)	Normal value
Idiopathic dilated cardiomyopathy	4	8	n.a.
Ischemic cardiomyopathy	3	7	n.a.
Age (years)	58.31±4.1	55.48±3.2	n.a.
Heart weight (grams)	368±121	455±114	275–330
Left ventricular systolic diameter (mm)	59±5	60±8	20–36
Left ventricular diastolic diameter (mm)	68±4	72±8	37–56
Wall thickness/chamber diameter	0.26±0.06	0.23±0.07	0.32–0.39
Ejection fraction (%)	20±5	22±6	>50
Cardiac output (mL/min)	3923±1284	4132±1059	5000–7000
Cardiac index ($mL \times min^{-1} \times (m^2)^{-1}$)	2375±689	2312±458	2600–4200
Pulmonary artery wedge pressure (mmHg)	19±3	22±4	1–10
Right ventricular end-diastolic pressure (mmHg)	12±9	13±7	0–8
Duration of disease (months)	121±26	74±17	n.a.
Onset of disease to heart failure (months)	91±53	65±32	n.a.
Time from heart failure to transplantation (months)	26±15	18±21	n.a.

Table 2. Demographical and clinical characteristics of control patients.

Variable	Female (n=5)	Male (n=6)	Normal value
Car accident resulting in head injury	3	4	n.a.
Ischemic stroke	2	1	n.a.
Aortic dissection	0	1	n.a.
Age (years)	48.54±3.9	51.23±2.8	n.a.
Heart weight (grams)	287±24	312±33	275–330

Results are presented as mean ± standard deviation. n.a. – not applicable.

The study was approved by the Institutional Review Board of the University of Verona and all patients selected gave informed consent prior to enrollment.

Myocardial samples were obtained from the hearts of 22 patients (7 female and 15 male) with ischemic cardiomyopathy (n=10) and idiopathic dilated cardiomyopathy (n=12) who underwent cardiac transplantation (Table 1). Among the patients with ischemic cardiomyopathy, 6 had a previous myocardial infarction and 7 underwent surgical revascularization.

All patients were medically treated with angiotensin converting enzyme (ACE) inhibitors, β-blockers, potassium sparing agents, and diuretics at maximal doses before transplantation. All patients had also received short-term intermittent treatment with intravenous inotropic agents at different stages.

All hearts were harvested in the surgical setting of cardiac transplantation and never post-mortem. The control hearts were collected from 11 patients (5 females and 6 males), who died from non-cardiac causes; control hearts were collected 1 hour to 6 hours after patient's death (Table 2).

Hemodynamic evaluation

Anatomical and functional properties of the failing hearts were measured by 2-dimensional echocardiography at 1 to 3 months before transplantation. Pressure measurements were determined by cardiac catheterization.

Tissue sampling and preparation

At the time of transplantation, tissue was removed from the left ventricular free wall and parceled into 3 portions. The first

Indexed in: [Index Medicus/MEDLINE] [EMBASE/Excerpta Medica] [Chemical Abstracts/CAS]

fragment part was fixed in 4% formaldehyde, stored at 4°C for a maximum of 48 hours, subsequently wax-embedded and finally used for immunofluorescent (IF), IHC, or hematoxylin and eosin (H and E) staining. The second fragment was collected into cryovials, snap-frozen in liquid nitrogen, stored at –80°C, and finally used for protein isolation from total tissue extracts. The third and last fragment was immediately fixed in buffered glutaraldehyde for electron microscopy.

Immunoblotting

Heart specimens were homogenized in lysis buffer (100 mmol/L NaCl, 0.1% Triton X-100, 50 mmol/L Tris; pH 8.3) loaded on 8% SDS-polyacrylamide gel, separated by gel electrophoresis, transferred onto a nitrocellulose membrane and probed with a relevant primary antibody.

Types and sources of the antibody used for the immunoblotting procedure are as follows: the antibody against α-actin (sc-32251), LC3-I (sc-134226), and LC3-II (sc-271625) were obtained from Santa Cruz Biotechnology (Santa Cruz, CA, USA). Secondary antibodies were conjugated to horseradish peroxidase and the ensuing immunoreactive bands were developed using a Western Lightning Chemiluminescence (WLC) kit (PerkinElmer Life Science, MA, USA). The nitrocellulose membrane used for western blotting was obtained from Bio-Rad Laboratories (Hercules, CA, USA). Immunoblots were digitalized and quantified using NIH ImageJ software (National Institute of Health, Bethesda, MD, USA).

Immunohistochemistry (IHC)

Autophagy was evaluated by immunostaining with a monoclonal antibody against LC3-II (sc-271625), while its relationship with apoptosis and necrosis was assessed by double-staining with a TUNEL assay kit (In Situ Cell Death Detection Kit, Roche Applied Science, IN, USA) and anti-C9 immune-staining (ab168345, from Abcam, Cambridge, MA, USA), respectively, used as a convenient tool for the detection of early oncosis in failing hearts [18,26,27]. Serial 5 µm myocardial sections were serially cut from the same wax blocks, stained with an LC3-II antibody, TUNEL reagents, or a C9 antibody according to manufacturer instructions, and subsequently incubated with appropriate fluorescent secondary antibodies (Dako Cytomation, Glostrup, Denmark), and finally counterstained with propidium iodide. To avoid autofluorescence of lipofuscin, the sections were stained with Sudan black before observation at confocal microscope. The percentage of co-localization of LC3-II positive staining with TUNEL or C9 positive labelling was digitally quantified by means of image analyzer software. Sections were analyzed by a confocal microscopist who was blinded to the origin and sequence of the specimens. Data were expressed as the means ± standard deviation (SD) of 12 to 15 high power fields.

In another set of experiments, sections were stained with anti-C3 antibody (Novus Biologicals, NB100-56113) diluted 1: 100, anti-NF-κB antibody (NB110-57266) diluted 1: 250, RIP3 antibody (Gene-Tex, GTX-107574) diluted 1: 100, and anti-RIP1 antibody (sc-133102, Santa Cruz Biotechnology Inc.) diluted 1: 100. The sections were visualized with a rabbit ABC-peroxidase staining system kit (Santa Cruz Biotechnology Inc.). The IHC of controls was performed omitting the primary antibody. The ABC-peroxidase staining intensity in IHC was evaluated using Image Pro Plus 4.5.1 image analysis program. The optical density (OD) was calculated for arbitrary areas, by measuring 10 fields for each sample.

On sections stained with anti-NF-κB, we also counted the percentage of immune stained nuclei. The number of anti-NF-κB stained nuclei present in 1 mm^2 was determined on randomly chosen areas at 400x magnification. From these data and the area of the tissue section, positive nuclei were expressed as a % of the total number.

Electron microscopy

The heart samples were fixed with 3% glutaraldehyde in cacodylate buffer (pH 7.4, 0.2 M) and post-fixed with 1% osmium tetroxide as previously described [28]. The pH was adjusted to 7.4 and the osmolarity to 330 milliosmoles per liter to assure dimensional stability of the specimens. Furthermore, the samples were processed with standard procedures for embedding in Araldite (Sigma-Aldrich Chemical Co., Milan, Italy). Thick sections (about 1 µm) were stained with Epoxy Tissue Stain (#14950, Electron Microscopy Sciences, PA, USA). The ultrathin sections (70 nm) were double-stained with a saturated aqueous solution of uranyl acetate and lead citrate and examined with a Philips CM10 electron microscope (Royal Philips Electronics, Amsterdam, The Netherlands) examining several different levels of each sample.

Statistical analysis

All results were expressed as mean ±SD. A *P*-value of 0.05 was considered statistically significant. For the molecular data, significance was evaluated using one- or two-way ANOVA followed by Student-Newman-Keuls post hoc tests, or *t*-tests as appropriate. For the baseline data and clinical characteristics, the continuous variables were first tested for normality using the Shapiro-Wilk test and then compared using the Student *t*-test or Mann-Whitney U test, accordingly. The categorical variables were compared using the Fisher's exact test and ordinal variables using the Mann-Whitney U test. Statistical analysis was assessed using the Statistical Package for Social Sciences program for Windows, version 25.0 (SPSS, Inc., Chicago, IL, USA).

Indexed in: [Index Medicus/MEDLINE] [EMBASE/Excerpta Medica] [Chemical Abstracts/CAS]

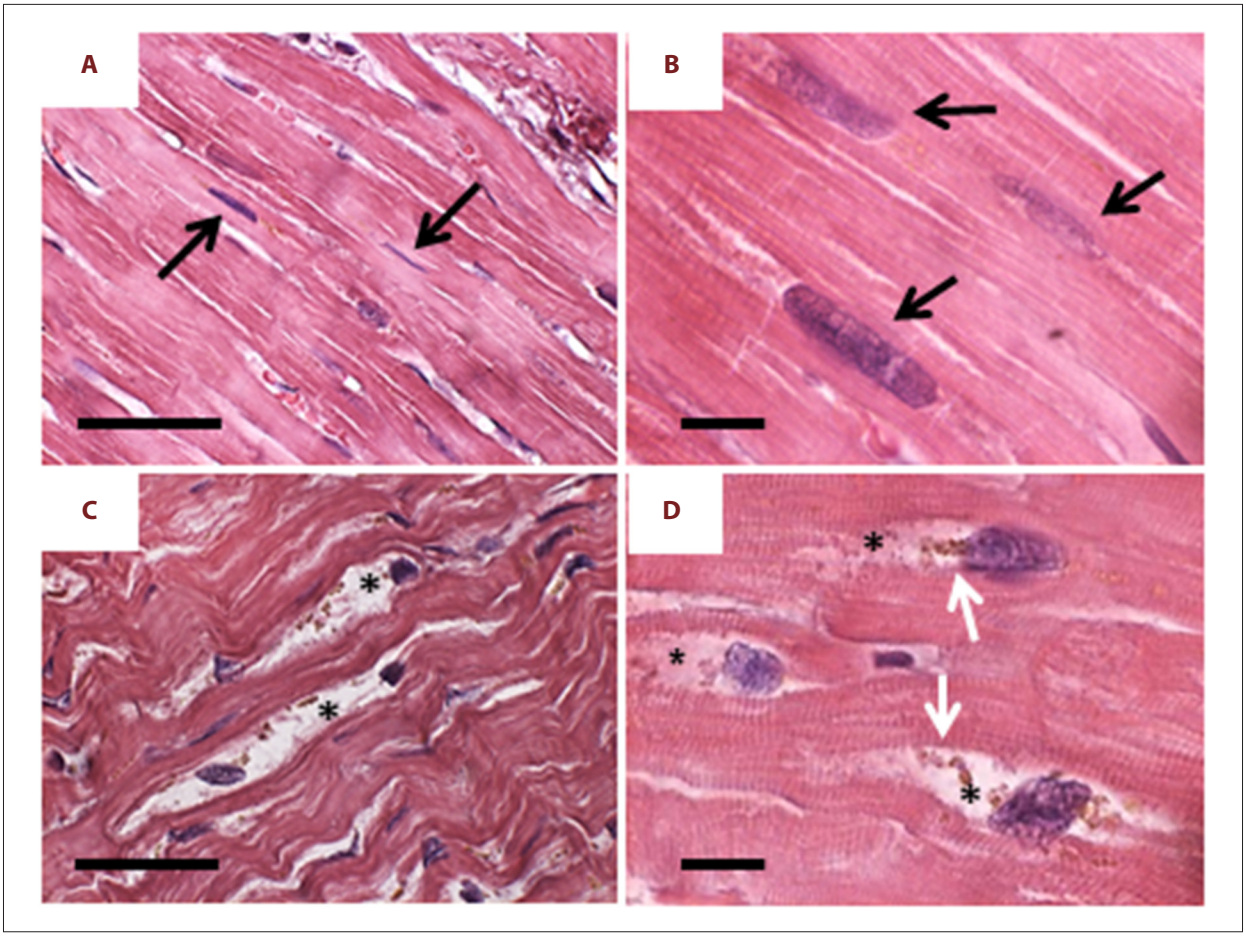

Figure 1. H and E staining. (**A, B**) Control heart: the cardiomyocytes show regular organization both at lower (**A**) and higher (**B**) magnification. The nuclei have regular elongate shape (arrows) and the myofibrils are compact. (**C, D**) Failing heart: already at lower magnification (**C**) many cardiomyocytes shows altered morphology. The nuclei are irregular in shape and shows "bite-like" signs. Around these nuclei, the cytoplasm is devoid of organelles (asterisks) and there are always clumps of lipofuscin-like brown granules (white arrows). Scale bar: **A** and **C**=20 µm; **B** and **D**=5 µm.

Results

Patients demographic and clinical data

The demographic and clinical data of patients studied are described in Table 1 and the control patients in Table 2.

Histopathology

With H and E staining, cardiomyocytes of the control hearts showed regular organization. The nuclei had consistent elongate shape and the myofibrils were compact (Figure 1A, 1B). Conversely, several cardiomyocytes from the failing hearts showed altered morphology. The nuclei were irregular in shape with bitten-like signs at one pole. Around these nuclei, mainly in proximity of the "bitten pole", large areas of empty cytoplasm containing clumps of brown granules were frequently observed (Figure 1C, 1D).

Increased autophagy in heart failure

LC3-II positive vacuolar staining was observed in 8.7±1.2% of myocytes in heart failure samples, compared with 1.2±0.3% of control hearts. In line with this finding, LC3 cleavage assessed by western blot analysis was 3.5-fold greater in failing hearts as compared to control hearts (Figure 2A). This was also confirmed by LC3-II IHC (Figure 2B–2D). There were no significant differences in the proportion of LC3-II positive cells in hearts from patients with ischemic cardiomyopathy compared with those with idiopathic dilated cardiomyopathy. We observed a repetitive progression of LC3-II staining, supporting the existence of multiple autophagy stages, exhibiting progressively severe morphological alterations progressively ingravescent, until cardiomyocytes cell death ensues. Indeed, the staining began at one cytoplasmic pole of the cardiomyocytes (Figure 3A, stage I) and extended to both poles (Figure 3B, stage II). Subsequently, the autophagy process radiated from the perinuclear region of the

Indexed in: [Index Medicus/MEDLINE] [EMBASE/Excerpta Medica] [Chemical Abstracts/CAS]

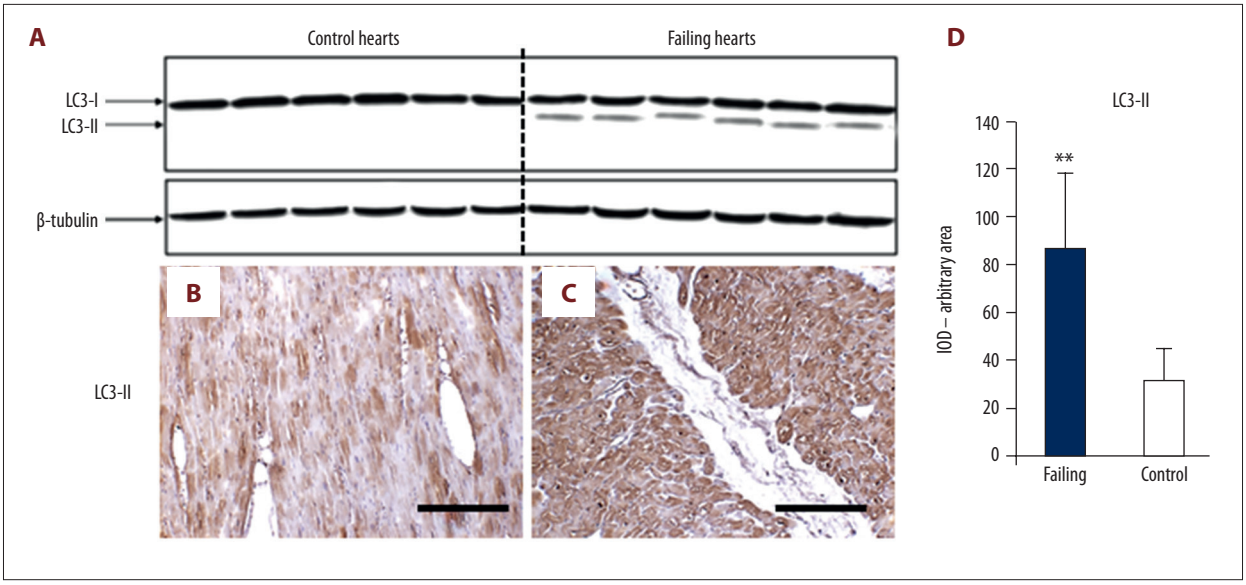

Figure 2. (**A**) Western blotting analysis for LC3-I and LC3-II. Cleaved LC3 is present in failing hearts only. (**B**) Anti-LC3-II IHC in control hearts: the cardiomyocytes show faint staining in small cytoplasm areas. (**C**) In failing hearts, the cardiomyocytes appear more intensely stained; scale bar 100 µm. The optical density for LC3-II staining is resumed in (**D**); ** *t*-test $P<0.000$. LC3 – light-chain-3 protein; IHC – immunohistochemistry.

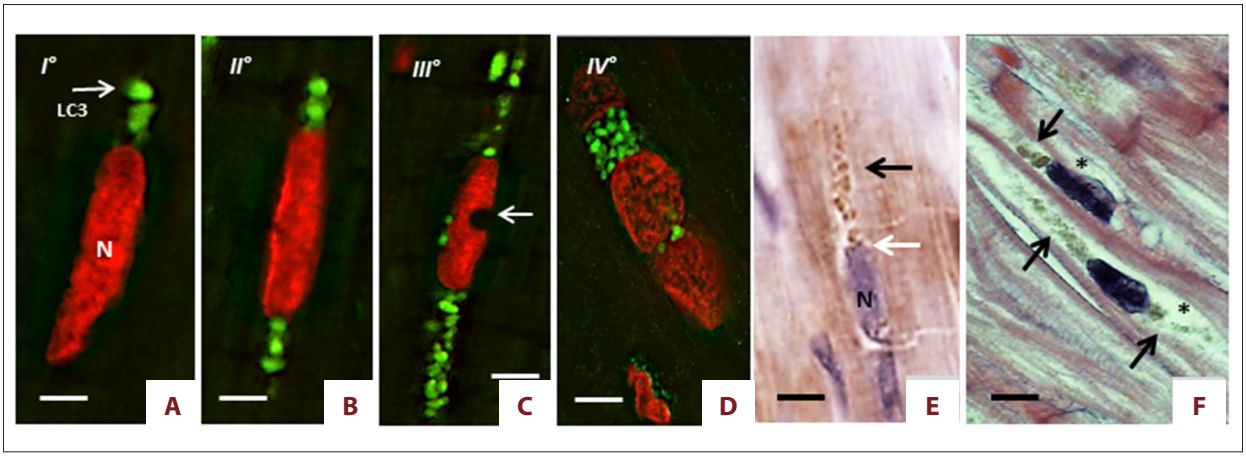

Figure 3. Representative progression of autophagy in failing heart. (**A**) Stage I: LC3-II staining (green) began at one cytoplasmic nuclear pole of the cardiomyocyte; N – nucleus, propidium iodide staining. (**B**) Stage II: the autophagy extended to both nuclear poles. The nuclei have normal appearance. (**C**) Stage III: the autophagy radiated to more peripheral cytosolic areas. The nuclei exhibit findings of focal compromise in form of single or multiple concavities (arrow) as "bite-like" signs. (**D**) Stage IV: in the later stages, the nucleus underwent progressive vacuolization and final disintegration. Cardiomyocytes with massive green staining in combination with the red staining of nucleus, assume a "strawberry-like" appearance. (**E**) Representative IHC for anti-LC3-II ABC-diaminobenzidine staining shows a massive presence of stained vacuoles (black arrow) that originated from a nuclear pole (white arrow), N – nucleus. (**F**) Representative H and E staining of later stages (III and IV) of autophagy progression. Unipolar and bipolar clustered granules of different size (arrows), the nuclei appear vacuolated and shows small bit signs. The cytoplasm is apparently empty (asterisks); white bar=5 µm; black bar=10 µm. LC3 – light-chain-3 protein; IHC – immunohistochemistry.

cytosol to more peripheral cytosolic areas. Despite the grossly normal appearance at the initial stages of the autophagic process, the nuclei displayed features of focal damage in the form of single or multiple concavities, probably expression of local erosion or digestion (bite-like signs) (Figure 3C, stage III). In the later stages, the nucleus underwent progressive vacuolization and final disintegration. At this advanced step of the process, the combination of LC3-II and propidium iodide staining gave the affected nuclei a peculiar "strawberry-like" appearance (Figure 3D, stage IV). This arbitrary subdivision in stages was

Indexed in: [Index Medicus/MEDLINE] [EMBASE/Excerpta Medica] [Chemical Abstracts/CAS]

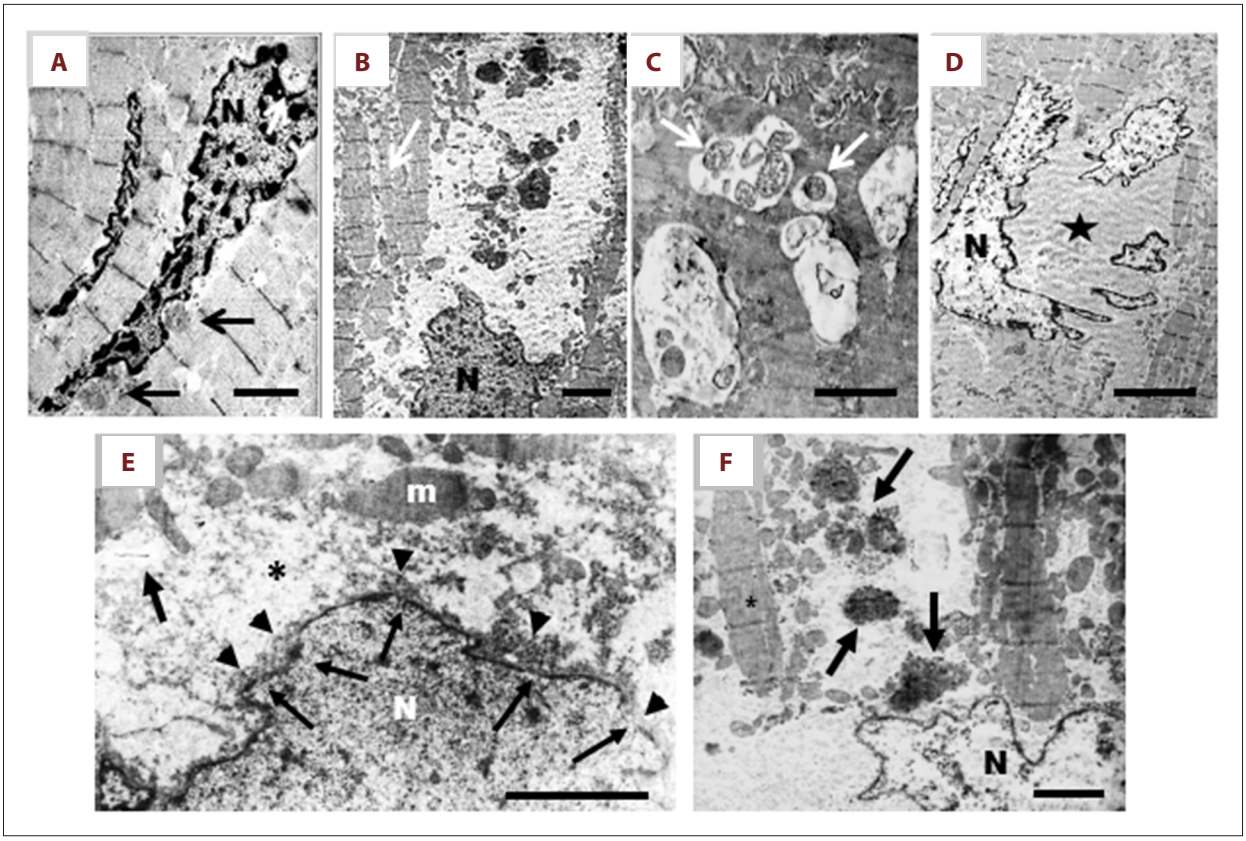

Figure 4. (**A–F**) Failing heart: representative electron microscopy pictures of cardiomyocytes alteration in advanced stages of damage. (**A**) Damaged cardiomyocytes sometime show nuclei with chromatin condensation, combined with invaginations of the nuclear envelope (arrows) that contain finely granular material cytoplasm without organelles. It is interesting to note the close similarity between this ultrastructural image and the nuclear concavities in Figure 3C; scale bar=2.5 µm. (**B**) The autophagy extends from the perinuclear areas to farther portion of cytosol. This is devoid of organelles and contains few small mitochondria and voluminous electron-dense material (probably lipofuscin and/or residue of autophagosomes) of variable size immersed in finely granular and faint electron-dense matrix. The myofibrils are isolated (arrow) and shown sign of disorganization; scale bar=3 µm. (**C**) Dilated vesicles of variable size containing mitochondria (arrows), and/or other unrecognizable residues were commonly observed; scale bar 1 µm. (**D**) At later stages the nucleus is fragmented, chromatin is condensed and marginated. Large cytoplasmic area devoid of organelles is evident (star); scale bar=5 µm. (**E**) The nuclear envelope is irregular with small interruptions (arrows) from which light-electron-dense nuclear material comes out (head arrows). Around the nucleus, there is evident a large area of cytoplasm devoid to organelles (asterisk); m – mitochondria; scale bar=1.5 µm. (**F**) At very advanced stage, nuclear content appears more electron-transparent. The cytoplasm is empty and very disorganized, many waste products are present (arrows) and myofibrils are isolate (asterisk); scale bar=2.5 µm; N – nucleus.

corroborated by histologic evaluation of the failing hearts by H and E and anti-LC3-II ABC-diaminobenzidine staining (Figure 3E, 3F). Likewise, the morphological changes in the autophagic process observed by optical microscopy were also confirmed by examination of the same failing hearts by electron microscopy (Figure 4A–4F).

Co-localization of autophagy and apoptosis

To evaluate whether autophagy could be associated with apoptosis, we performed immunofluorescence with both LC3-II and TUNEL, counterstaining the DNA with Topro 3. Figure 5A–5C shows that LC3-II positive areas co-localize with TUNEL staining, suggesting that both autophagy and apoptosis occur simultaneously in the same dying cells. TUNEL fluorescent positivity was observed in vesicles seemingly originating from the nucleus, which shows erosions with a typical bite-like appearance. This finding suggests that DNA fragments were present in all vesicles. Since tissue sections were stained with Sudan black to eliminate the auto-fluorescence of lipofuscin, the observed TUNEL positivity is a reliable apoptosis marker. In order to confirm the localization of TUNEL, we also performed IHC for C3. Intense anti-C3 staining was observed inside the cytoplasmic vesicles and nuclei of failing heart cardiomyocytes,

Indexed in: [Index Medicus/MEDLINE] [EMBASE/Excerpta Medica] [Chemical Abstracts/CAS]

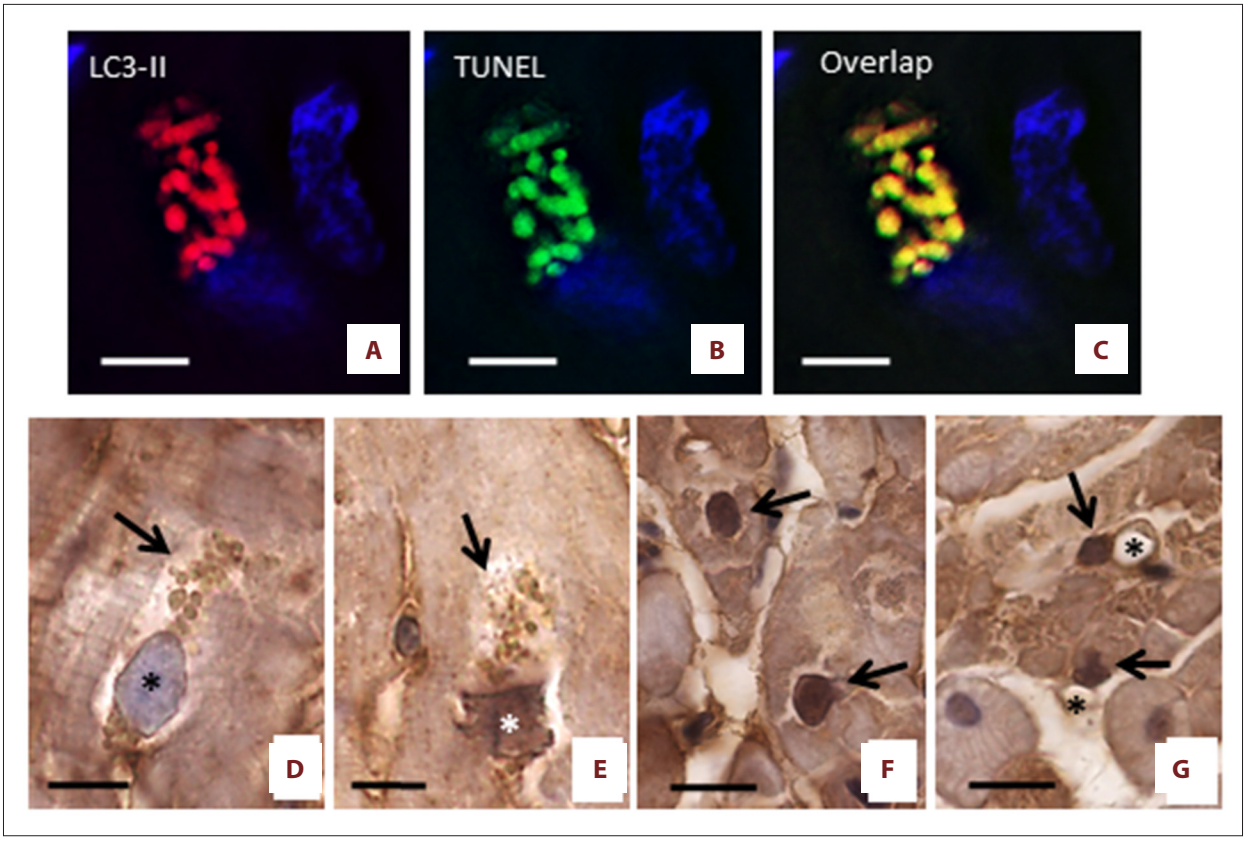

Figure 5. Co-localization of autophagy and apoptosis. (**A–C**) LC3 positive areas co-localize with the TUNEL, suggesting that both autophagy and apoptosis are present simultaneously in damaged cells. The sections were stained with Sudan black to delete the auto-fluorescence of lipofuscin. The nuclei are in blue. (**D–G**) Representative progression of apoptosis (ABC-diaminobenzidine IHC for active-C3) in failing heart. (**D**) the nuclear rim appears to be slightly irregular and a slight staining is observed on the inner surface of the nuclear envelope (asterisk). At the nuclear poles there are numerous large vesicles with pale staining(arrow). (**E**) In the later stage of autophagic alteration, the vesicles (arrows) seem to originate from nucleus, are small and show a more intense staining. The nuclear pole from which the vesicles seem to originate appears truncated. Inside the IHC staining is moderate (asterisks). (**F**) Intense anti-C3 stained nuclei of cardiomyocytes from heart failure patients. These nuclei did not show "bite signs", or cytoplasmic vesicles. (**G**) Non-cardiomyocytes cell nuclei (arrow) near at vessel (asterisk) were sometime seen in heart failure patients. Scale bar=10 µm. IHC – immunohistochemistry; C3 – cleaved-caspase-3.

undergoing the final stage of the autophagy process. Of note, these nuclei had one pole apparently regular in shape, whereas the opposite pole appeared to be strongly damaged, as if it had been "eaten into" TUNEL and anti-C3 positive staining started to become evident at the periphery of the affected nuclei as well as in the vesicles, which appeared to be detached from the same nuclei and accumulate in the surrounding cytosolic areas (Figure 5D, 5E). Occasionally, the nuclei of cardiac cells from failing hearts exhibited homogenously intense anti-C3 staining. For unclear reasons, such nuclei did not present evident erosions ("bite-like" signs), perhaps because they were not included in the section plan, and/or stained vesicles in the perinuclear cytoplasm (Figure 5F). Anti-C3 staining was seldom observed in cells other than myocytes from the failing hearts (Figure 5G).

Autophagy was also associated with features of oncosis and necroptosis

To test whether late stage cells from heart failure samples could jointly exhibit features of autophagy and oncosis, we stained the cells with LC3-II and with antibodies recognizing complement C9. Figure 6 portrays a myocyte showing co-localization of LC3-II and C9 staining. It should be noted that while the LC3-II staining was vesicle-based, the C9 staining was evenly spread throughout the cell. This would suggest that the activation of the oncotic process takes place simultaneously all over the cell.

To corroborate these observation, we also evaluated by IHC in serial sections of heart failure hearts and control hearts, the expression of the necroptosis markers RIP1 and RIP3. Failing hearts

Indexed in: [Index Medicus/MEDLINE] [EMBASE/Excerpta Medica] [Chemical Abstracts/CAS]

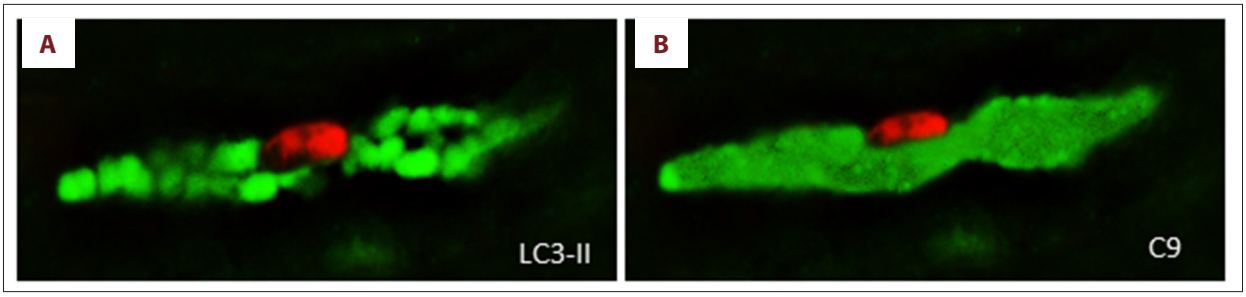

Figure 6. Co-localization of autophagy (**A**) and oncosis (**B**). Representative pictures of cell showing generalized cytoplasmic LC3-II staining also show intense C9 reactivity. However, it should be noted that while the LC3-II staining were concentrated in separated oval areas with different intensity, the C9 staining is evenly spread throughout the cell. Nuclei are in red. Scale bar=10 µm. LC3 – light-chain-3 protein; C9 – complement 9.

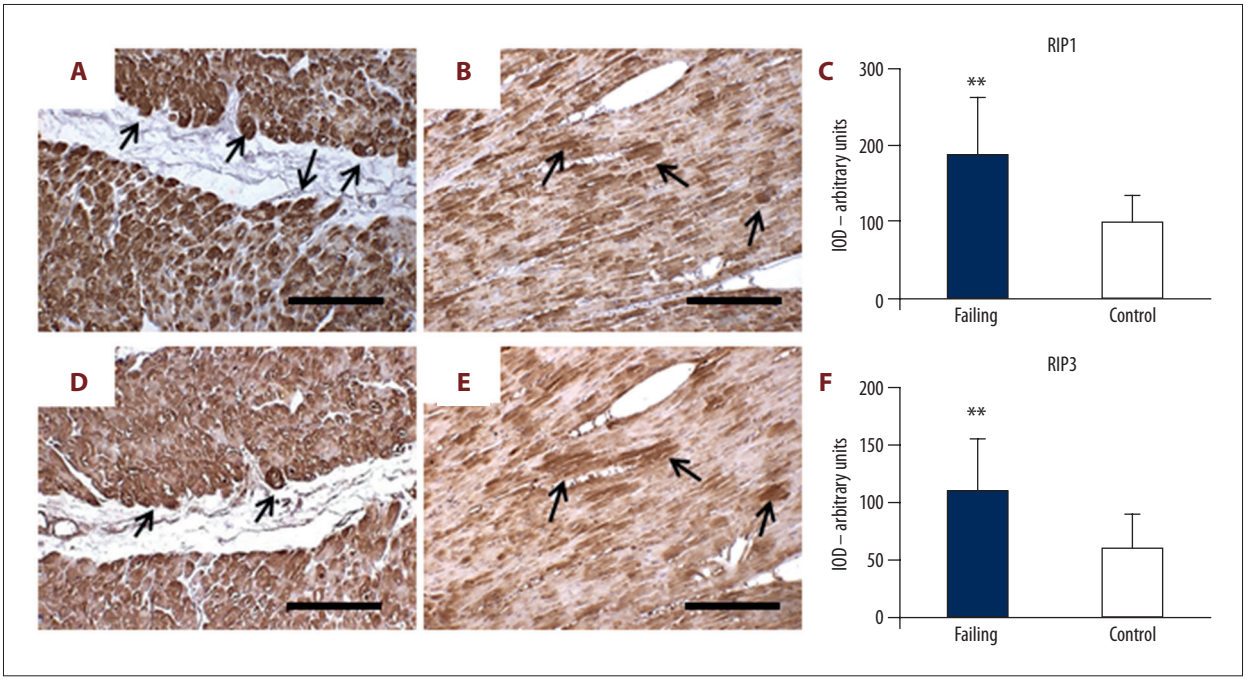

Figure 7. Serial sections with anti-RIP1 and anti-RIP3 immunostaining. (**A–C**) RIP1 in failing heart (**A**) shows strong and diffuse staining. Some cardiomyocytes are very strongly stained (arrows). Control heart (**B**) shows faint and very scarce staining. Only small cytoplasmic areas are moderately stained. The optical density for RIP1 staining is resumed in (**C**). (**D–F**) RIP3 in failing heart (**D**): the cardiomyocytes that appear strongly RIP3-stained (arrows) correspond those strongly RIP1 stained. Control heart (**B**), the cardiomyocytes shows moderate staining in small cytoplasm areas that overlap those stained with RIP1. The optical density for RIP3 staining is resumed in (**F**). Scale bars=100 µm, ** *t*-test, $P<0.000$. RIP1 – receptor interacting protein kinase 1; RIP3 – receptor interacting protein kinase 3.

showed a significant increase in RIP1 positive staining. Almost all cardiomyocytes were intensely and diffusely stained, although some cells showed a more intense positivity. Conversely, control hearts showed only faint and very scarce staining. Only a few cells presented with weak positivity in small areas of the cytosol (Figure 7A–7C). Likewise, RIP3 positive staining increased significantly in the failing hearts and was seen to co-localize with RIP1 labeling in the positive myocytes. Such co-localization was also observed in the few RIP1/RIP3 positive cardiac cells from the control hearts (Figure 7D–7F).

Finally, in order to evaluate potential inflammatory alterations in cardiomyocytes, we assessed the expression level of NF-κB in cardiac sections from heart failure patients (Figure 8A–8C). Intensely positive staining for NF-κB was observed not only in the cytosol, but also in the nucleus of several cardiomyocytes from failing heart samples (Figure 8A, 8C). Sometimes, the NF-κB positive nuclei showed large "bite-like" erosions at pole extremities (Figure 8A inserts). Conversely, NF-κB staining was sporadic and faint in cardiac myocytes from control heart samples. Such positive staining was almost exclusively seen in

Indexed in: [Index Medicus/MEDLINE] [EMBASE/Excerpta Medica] [Chemical Abstracts/CAS]

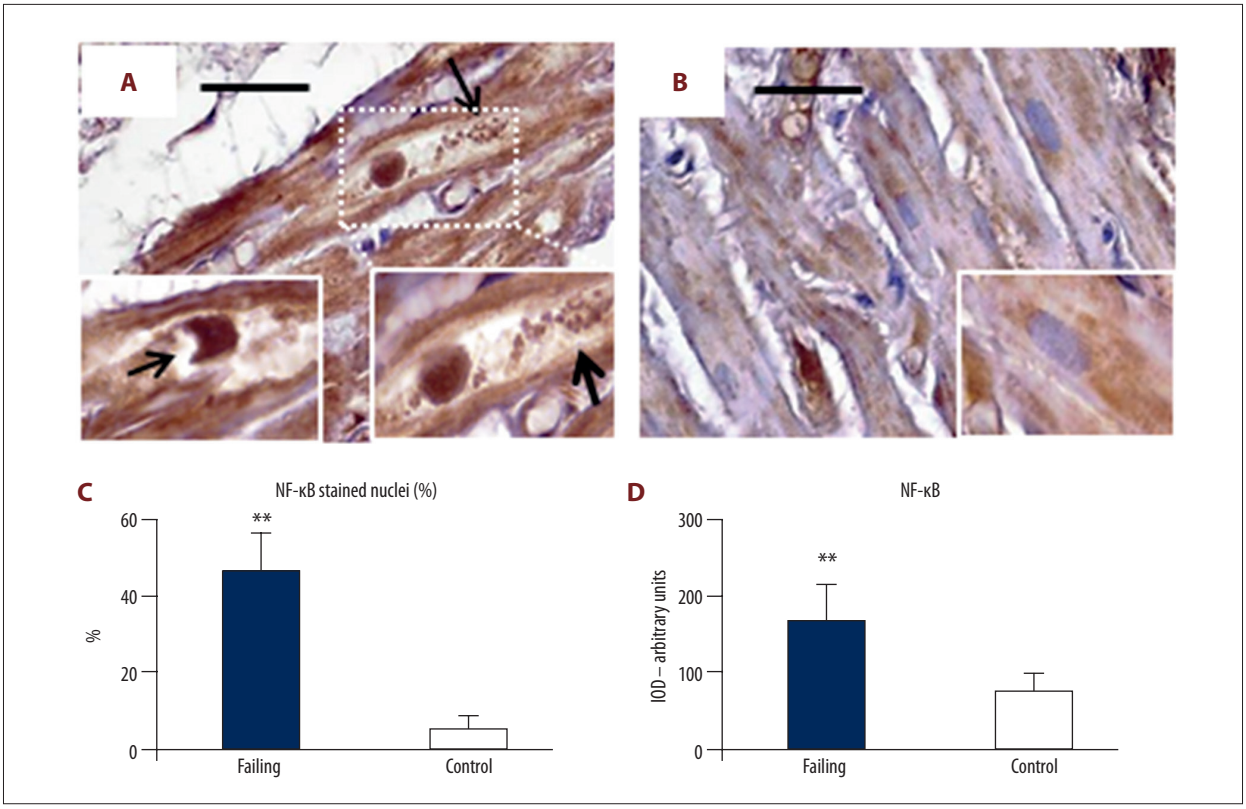

Figure 8. NF-κB immunostaining. (**A**) Cardiomyocytes in failing heart had intense NF-κB staining distributed not only inside large cytoplasm areas, but also in a large proportion of nuclei. The cytoplasm appears empty with a lot of debris product (arrows, right insert). The nuclei sometimes showed large "bite-like" signs at pole extremities (arrow in left insert). Conversely (**B**, and insert), NF-κB was faintly expressed inside the small cytoplasmic areas of control heart samples. The quantitative data of stained nuclei are shows in (**C**). The optical density for NF-κB staining is resumed in (**D**). Original magnification 200×; scale bar 30 μm; ** *P*<0.01. NF-κB – nuclear factor kappa-light-chain-enhancer of activated B cells.

small areas of the cytosol (Figure 8B and insert), while nuclei were seldom immunostained (Figure 8C). The optical density for NF-κB staining is presented in Figure 8D.

Discussion

The main aim of this study was to assess the status and progression of autophagy and oncosis/necroptosis, in the *ex vivo* heart of patients with intractable heart failure. Indeed, a characteristic feature of heart failure is progressive loss of cardiac myocytes and development of cardiac dysfunction. So, the identification of the main mechanisms leading to progressive myocyte cell death could provide a valuable base for the development of clinically useful therapeutic intervention.

Autophagy is an intracellular lysosome-mediated catabolic mechanism responsible for the bulk degradation and recycling of damaged or dysfunctional cytoplasmic components and organelles [29]. Although autophagy is fundamental for cellular homeostasis, higher autophagy rates can result in cell death secondary to cell cannibalization. Indeed, autophagy is associated with many pathological states such as cancer, neurodegenerative disorders, myopathies, and cardiomyopathies [27].

Detection of LC3-positive structures, either by immunostaining of endogenous LC3 or localization of transfected GFP-LC3, is the most commonly used method to detect autophagosomes by light microscopy. However, electron microscopy analysis is required to demonstrate the direct sequestration of LC3 aggregates by autophagosomes [30,31].

Our results showed that autophagy, unlike apoptotic cell death, was largely present in failing heart cardiomyocytes. The early detection by electron microscopy of numerous autophagosomes in cardiomyocytes from heart failure patients indicated that autophagocytosis was a relevant process driving cardiomyocytes to death.

Furthermore, our study has shown that the progression of autophagy occurs according to a set sequence, traversing 4 progressive phases (from I to IV). Our findings indicate that the

Indexed in: [Index Medicus/MEDLINE] [EMBASE/Excerpta Medica] [Chemical Abstracts/CAS]

nucleus is an early autophagic target and develops typical erosions with a bite-like appearance. Remarkably, in the most advanced stages of the process, the autophagic vacuoles, in addition to LC3 positivity, develop TUNEL positivity, suggesting that their content is represented by DNA fragments eaten away from the nucleus. Myocytes exhibiting combined LC3 and TUNEL positive staining acquire a peculiar "strawberry-like appearance", which is morphologically original and has never been previously described. In addition, our data demonstrated that autophagy was accompanied by oncosis, especially in the terminal phases of the autophagic process. The autophagic myocytes undergoing oncosis did not show dramatic cytoplasmic and/or nuclear abnormalities, which suggests an early stage of the process.

Programmed necrosis, also called necroptosis, is a caspase-independent RIP3-mediated form of cell death, which has recently been identified as a novel mechanism of cell death implicated in the pathogenesis of pathological conditions affecting different organs and apparatuses [32]. Our findings revealed enhanced RIP3 expression in cardiac cells from the human failing heart. This is in line with published data showing that RIP3 overexpression in the mouse heart can induce myocardial infarction, while the formation of RIP1/RIP3 complex can drive cardiomyocytes to necrosis [33].

Activation of RIP3 is regulated by the kinase RIP1 [34], a key player in the modulation of cell fate in response to different stimuli [35]. We documented increased expression of the pro-necroptotic proteins RIP3 and RIP1 in the human heart undergoing end-stage heart failure, which indicates the occurrence of both necroptosis activation and execution. Since RIP3/RIP1 overexpression was seen to frequently occur in LC3 positive myocytes, and only occasionally in LC3 negative cells, we postulated that necroptosis was chiefly triggered after initiation of autophagy. Our findings corroborated the results of a recent study that showed that human hearts with chronic heart failure secondary to myocardial infarction or dilated cardiomyopathy were positive for markers of necroptosis [36]. Although RIP1 is known to mediate cell death in response to DNA damage, it is also crucial for cell survival through activation of the NF-κB pathway [37]. Indeed, the anti-apoptotic activity of NF-κB may avoid unnecessary and/or redundant cell death in response to apoptotic stimuli such as TNF-α activation [24]. Accordingly, our findings documented that myocytes overexpressing both RIP1 and nuclear NF-κB, were TUNEL and RIP3 negative, suggesting that the RIP1/NF-κB pathway serves as an efficient survival pathway in the failing human heart.

Although rare in normal human myocardium (0.01–0.001%), the occurrence of apoptosis in human myocytes from failing hearts appears to be slightly higher (0.12–0.70%) [38]. Apoptosis has also been shown to be involved in acute and chronic loss of cardiomyocytes occurring in myocardial infarction, ischemic heart disease, reperfusion injury, and various forms of cardiomyopathy [39,40]. More recent findings have demonstrated that in human and monkey failing hearts, the rate of apoptosis in non-cardiomyocytes was higher than cardiomyocytes [41]. In line with such studies, we observed a low expression of pro-apoptotic markers in both cardiomyocytes and non-cardiomyocytes from failing hearts. Taken together, our data suggest that apoptosis, in comparison to autophagy and oncosis/necroptosis, is neither the earliest nor the main type of cell death detected in cardiomyocytes from heart failure patients.

In this work, we predominantly focused on the morphological aspects of cell death occurring in the setting of advanced heart failure in humans. To this end, we relied almost exclusively on IHC, whose limitations represent the major weakness of the current work. Indeed, the soundness of IHC is operator-dependent, requiring rigor of execution (to prevent technical errors potentially leading to misinterpretation) and analytical skills (to minimize the risk of bias). The longstanding experience of the operators in the specific field of IHC should vouch for the scientific accuracy of the data presented in our work.

Conclusions

In conclusion, our study showed for the first time that in the failing human heart autophagy precedes and sets the stage for the occurrence of apoptosis, oncosis, and necroptosis, which only rarely start independently from autophagy. Hence, autophagy seems to be a primary driving force leading to the progressive cardiomyocyte cell loss observed in end-stage heart failure.

Abbreviations

C3 – cleaved-caspase 3; C9 – complement factor 9; LC3 – microtubule associated protein light chain 3; RIP1 – receptor-interacting serine/threonine-protein kinase 1; RIP3 – receptor-interacting serine/threonine-protein kinase 3; NF-κB: nuclear factor kappa-light-chain-enhancer of activated B cells; TUNEL – terminal deoxynucleotidyl transferase – mediated deoxyuridine triphosphate nick end labeling.

Indexed in: [Index Medicus/MEDLINE] [EMBASE/Excerpta Medica] [Chemical Abstracts/CAS]

References:

1. Garg S, Narula J, Chandrashekhar Y: Apoptosis and heart failure: Clinical relevance and therapeutic target. J Mol Cell Cardiol, 2005; 38(1): 73–79
2. Chiong M, Wang ZV, Pedrozo Z et al: Cardiomyocyte death: Mechanisms and translational implications. Cell Death Dis, 2011; 2: e244
3. Kostin S: Pathways of myocyte death: Implications for development of clinical laboratory biomarkers. Adv Clin Chem, 2005; 40: 37–98
4. Hein S, Arnon E, Kostin S et al: Progression from compensated hypertrophy to failure in the pressure-overloaded human heart: Structural deterioration and compensatory mechanisms. Circulation, 2003; 107(7): 984–91
5. De Meyer GRY, De Keulenaer GW, Martinet W: Role of autophagy in heart failure associated with aging. Heart Fail Rev, 2010; 15(5): 423–30
6. Zhang Z, Li H, Chen S et al: Knockdown of microRNA-122 protects H9c2 cardiomyocytes from hypoxia-induced apoptosis and promotes autophagy. Med Sci Monit, 2017; 23: 4284–90
7. Kanamori H, Takemura G, Goto K et al: Autophagy limits acute myocardial infarction induced by permanent coronary artery occlusion. Am J Physiol Heart Circ Physiol, 2011; 300(6): H2261–71
8. Klionsky DJ, Emr SD: Autophagy as a regulated pathway of cellular degradation. Science, 2000; 290: 1717–21
9. Kabeya Y, Mizushima N, Ueno T et al: LC3, a mammalian homologue of yeast Apg8p, is localized in autophagosome membranes after processing. EMBO J, 2000; 19: 5720–28
10. Kuma A, Hatano M, Matsui M et al: The role of autophagy during the early neonatal starvation period. Nature, 2004; 432(7020): 1032–36
11. Chen-Scarabelli C, Agrawal PR, Saravolatz L et al: The role and modulation of autophagy in experimental models of myocardial ischemia-reperfusion injury. J Geriatr Cardiol, 2014; 11(4): 338–48
12. Liu X, Van Vleet T, Schnellmann RG: The role of calpain in oncotic cell death. Annu Rev Pharmacol Toxicol, 2004; 44: 349–70
13. Kanamori H, Takemura G, Goto K et al: Autophagy limits acute myocardial infarction induced by permanent coronary artery occlusion. Am J Physiol Heart Circ Physiol, 2011; 300(6): H2261–71
14. Lum JJ, Bauer DE, Kong M et al: Growth factor regulation of autophagy and cell survival in the absence of apoptosis. Cell, 2005; 120(2): 237–48
15. Lee YK, Lee JA: Role of the mammalian ATG8/LC3 family in autophagy: Differential and compensatory roles in the spatiotemporal regulation of autophagy. BMB Rep, 2016; 49(8): 424–30
16. Majno G, Joris I: Apoptosis, oncosis, and necrosis. An overview of cell death. Am J Pathol, 1995; 146(1): 3–15
17. Peitsch MC, Tschopp J: Assembly of macromolecular pores by immune defense systems. Curr Opin Cell Biol, 1991; 3(4): 710–16
18. Doran JP, Howie AJ, Townend JN: Detection of myocardial infarction by immunohistological staining for C9 on formalin fixed, paraffin wax embedded sections. J Clin Pathol, 1996; 49: 34–37
19. Kanduc D, Mittelman A, Serpico R et al: Cell death: Apoptosis versus necrosis (review). Int J Oncol, 2002; 21: 165–70
20. Adameova A, Goncalvesova E, Szobi A, Dhalla NS: Necroptotic cell death in failing heart: relevance and proposed mechanisms. Heart Fail Rev, 2016; 21(2): 213–21
21. Hinz M, Krappmann D, Eichten A et al: NF-kappaB function in growth control: Regulation of cyclin D1 expression and G0/G1-to-S-phase transition. Mol Cell Biol, 1999; 19(4): 2690–98
22. Baichwal VR, Baeuerle PA: Activate NF-κB or die? Curr Biol, 1997; 7(2): R94–96
23. Beg AA, Baltimore D: An essential role for NF-kappaB in preventing TNF-alpha-induced cell death. Science, 1996; 274(5288): 782–84
24. Kaltschmidt B, Kaltschmidt C, Hofmann TG et al: The pro- or anti-apoptotic function of NF-kappaB is determined by the nature of the apoptotic stimulus. Eur J Biochem, 2000; 267(12): 3828–35
25. Heidenreich P: Inflammation and heart failure: Therapeutic or diagnostic opportunity? J Am Coll Cardiol, 2017; 69(10): 1286–87
26. Ferreira MAS, Owen HE, Howie AJ: High prevalence of acute myocardial damage in a hospital necropsy series, shown by C9 immunohistology. J Clin Pathol, 1998; 51: 548–51
27. Kostin S, Pool L, Elsässer A et al: Myocytes die by multiple mechanisms in failing human hearts. Circ Res, 2003; 92(7): 715–24
28. Corsetti G, Pasini E, Scarabelli TM et al: Decreased expression of Klotho in cardiac atria biopsy samples from patients at higher risk of atherosclerotic cardiovascular disease. J Geriatr Cardiol, 2016; 13(8): 701–11
29. Dunn JWA: Autophagy and related mechanisms of lysosome mediated protein degradation. Trends Cell Biol, 1994; 4: 139–43
30. Szeto J, Kaniuk NA, Canadien V et al: ALIS are stress-induced protein storage compartments for substrates of the proteasome and autophagy. Autophagy, 2006; 2: 189–99
31. Kuma A, Matsui M, Mizushima N: LC3, an autophagosome marker, can be incorporated into protein aggregates independent of autophagy: Caution in the interpretation of LC3 localization. Autophagy, 2007; 3(4): 323–28
32. Weinlich R, Oberst A, Beere HM, Green DR: Necroptosis in development, inflammation and disease. Nat Rev Mol Cell Biol, 2017; 18(2): 127–36
33. Luedde M, Lutz M, Carter N et al: RIP3, a kinase promoting necroptotic cell death, mediates adverse remodelling after myocardial infarction. Cardiovasc Res, 2014; 103(2): 206–16
34. Newton K, Dugger DL, Maltzman A et al: RIPK3 deficiency or catalytically inactive RIPK1 provides greater benefit than MLKL deficiency in mouse models of inflammation and tissue injury. Cell Death Differ, 2016; 23(9): 1565–76
35. Hänggi K, Vasilikos L, Valls AF et al: RIPK1/RIPK3 promotes vascular permeability to allow tumor cell extravasation independent of its necroptotic function. Cell Death Dis, 2017; 8(2): e2588
36. Szobi A, Gonçalvesová E, Varga Z et al: Analysis of necroptotic proteins in failing human hearts. J Transl Med, 2017; 15: 86
37. Skaug B, Jiang X, Chen ZJ: The Role of ubiquitin in NF-κB regulatory pathways. Annu Rev Biochem, 2009; 78: 769–96
38. Van Empel VP, Bertrand AT, Hofstra L et al: Myocyte apoptosis in heart failure. Cardiovasc Res, 2005; 67: 21–29
39. Kang PM, Izumo S: Apoptosis and heart failure: A critical review of the literature. Circ Res, 2000; 86: 1107–13
40. Olivetti G, Abbi R, Quaini F et al: Apoptosis in the failing human heart. N Engl J Med, 1997; 336: 1131–41
41. Park M, Shen YT, Gaussin V et al: Apoptosis predominates in nonmyocytes in heart failure. Am J Physiol Heart Circ Physiol, 2009; 297(2): H785–91

Indexed in: [Index Medicus/MEDLINE] [EMBASE/Excerpta Medica] [Chemical Abstracts/CAS]